Coarse-grained Monte Carlo simulations of nanogel-polyelectrolyte complexes: electrostatic effects.

Luis Pérez-Mas[1,2], Alberto Martín-Molina[2,3], and Manuel Quesada-Pérez[1]*

[1]Departamento de Física, Escuela Politécnica Superior de Linares, Universidad de Jaén, 23700, Linares, Jaén, Spain

[2]Departamento de Física Aplicada, Universidad de Granada, Campus de Fuentenueva sn, 18071 Granada, Spain

[3]Instituto Carlos I de Física Teórica y Computacional, Universidad de Granada, Campus de Fuentenueva sn, 18071 Granada, Spain

Abstract.

Coarse-grained Monte-Carlo simulations of nanogel-polyelectrolyte complexes have been carried out. The results presented here capture two phenomena reported in experiments with real complexes: i) the reduction in size after absorbing just a few chains; ii) the charge inversion detected through electrophoretic mobility data. Our simulations reveal that charge inversion occurs if the polyelectrolyte charge is large enough. In addition, the distribution of chains inside the nanogel strongly depends on whether charge inversion takes place. It should be also stressed that the chain topology has very scarce influence on most of the properties studied here.

INTRODUCTION

Nanogels are crosslinked polymer (or polyelectrolyte) networks with sizes of just a few tens of nanometers.[1,2] One of their more outstanding characteristics is that these colloidal particles are able to swell or shrink in response to environmental properties, such as temperature or pH. As a result of this responsiveness and their high loading capacity, nanogels are very promising as drug-delivery carriers.[3–8] In particular, ionic nanogels can incorporate oppositely charged macromolecules, polyelectrolytes or inorganic nanoparticles due to attractive electrostatic forces. In fact, this principle can be exploited to immobilize oligonucleotides and plasmid DNA in cationic nanogels, which protect such polyelectrolytes from enzymatic degradation.[9–17] In addition, these nanogels can be used to deliver genes into a cell. Apart from that, nanogels have been proposed as a soft and porous alternative to solid substrates and, what is more, some research groups have experimentally investigated the absorption of some polyelectrolytes (such as poly(diallydimethylammoniumchloride) (PDADMAC), miktoarm star polymers, peptides or polystyrene suphonate) into micro- or nanogels.[18–23]

In order to control the uptake of polyelectrolytes by nanogels, we should fully understand the role played by electrostatic interactions, which are present in all charged systems. However, some counterintuitive electrostatic phenomena continue challenging many theorists of colloid science and soft matter. Widely known examples of this are charge inversion and the existence of attractive electrostatic forces between like-charged macroions. Strong electrostatic correlations and charge fluctuations neglected by mean-field theories are responsible in many cases for such striking phenomena.[24–29]

It is appropriate to mention in this regard that coarse-grained simulations of nanogels are particularly useful to consider these and other aspects which are not included in many theoretical models, such as the presence of nodes in the polyelectrolyte network or the

flexibility of the chains. In addition, these simulations have significantly contributed to elucidate some aspects of the behavior of nanogels,[30–47] such as size and charge effects. For instance, a previous work has recently showed that the deswelling and charge inversion observed after the absorption of spherical hard nanoparticles into nanogels can be explained in terms of electrostatic and excluded volume interactions.[48] The simulations performed therein also revealed that: i) charge inversion only takes place if the nanoparticle charge is large enough; ii) the distribution of hard nanoparticles inside the nanogel depends on whether charge inversion occurs.

Some experimental works assume that the formation of polyelectrolyte-microgel complexes is driven largely by electrostatic interactions to draw some conclusions about the role of these interactions.[20,22] In real systems, however, the presence of other interactions depending on the specific chemical nature of the microgel and polyelectrolyte chains is very likely. Commonly, such interactions are not known a priori and therefore it is difficult to reach firm conclusions. In this respect, computer simulations can be extremely helpful since they employ tailor-made systems, whose structure and interactions between their constituents are specified at the beginning.

According to the preceding paragraphs, one of the main goals of this work is to find out the precise role played by electrostatic forces in complexes formed by nanogels and soft polyelectrolyte chains incorporated into them. To tackle this issue, the absorption of linear and ring polyelectrolyte chains into nanogels has been simulated using the bead-spring model for both species. In this way, the complex topology of nanogels and the fluctuations of polyelectrolyte chains are explicitly considered. Different properties of the polyelectrolyte/nanogel complexes formed are analyzed paying special attention to size and charge effects. Linear and ring polyelectrolyte chains are inspired in oligonucleotides and plasmid DNA, since the latter it has been proved to be much more efficiently

transfected than linear DNA (when cationic lipids as used as vectors in gene therapy).[49,50] However, the results obtained here go far beyond DNA arrangements and can be relevant for a huge variety of polyelectrolyte/nanogel complexes given the generality of the model. Apart from this, ring polymers were also included in our study because two polyelectrolytes with the same charge but different architecture or topology exhibit different charge distributions. Therefore, the comparison between ring and linear polyelectrolytes will help us discover if the chain charge distribution has important effects.

MODEL AND SIMULATIONS

The coarse-grained picture employed here for polyelectrolyte chains and nanogels is the so-called bead-spring model. According to this representation of reality, monomer units and ions are modeled as spheres, whereas the solvent is modeled as a dielectric continuum. The short-range repulsion between any pair of beads (monomers or ions) due to excluded volume effects is modeled by means of the Weeks–Chandler–Andersen potential:

$$u_{LJ}(r) = \begin{cases} 4\varepsilon_{LJ}\left(\frac{d^{12}}{r^{12}} - \frac{d^{6}}{r^{6}} + \frac{1}{4}\right) & r \le \sqrt[6]{2}(a_i + a_j) \\ 0 & r > \sqrt[6]{2}(a_i + a_j) \end{cases} \quad (1)$$

Here r is the center-to-center distance between a given pair of particles, ε_{LJ}=4.11·10^{-21} J, a_i stands for the radius of species i and $d = a_i + a_j$. We assumed that the monomers of the nanogel and the monomers of the free chains have similar but slightly different diameters (d = 0.65 and 0.7 nm, respectively). Estimates of the diameters of different monomers yield values of this order.[51] A diameter of 0.7 nm was also employed for ions. The hydration shell of ions is included in the corresponding spheres.

Consecutive monomers of a chain are connected by harmonic bonds, whose interaction potential is:

$$u_{bond}(r) = 0.5k_{bond}(r - r_0)^2 \quad (2)$$

where k_{bond} is the elastic constant and r_0 is the equilibrium length corresponding to this harmonic potential. The r_0-values used for monomers of the nanogel and the free polyelectrolyte chains were identical to their respective diameters, but the same k_{bond}-value was employed for both, 0.4 N/m. This value was also employed by Schneider and Edgecombe *et al.* in coarse-grained simulations of polyelectrolyte gels.[52–54] Other authors proposed elastic constants much greater than k_BT/d_m^2, where d_m is the diameter of monomers, k_B is Boltzmann's constant and T the absolute temperature.[30,55] This ensures that thermal fluctuations undergone by monomers are much smaller than their diameter. The elastic constant employed in this work also satisfies this condition.

Some monomers of the free polyelectrolyte chains and nanogels carry electric charge. These beads and ions interact through the Coulomb potential:

$$u_{elec}(r) = \frac{Z_i Z_j e^2}{4\varepsilon_0 \varepsilon_r r} \quad (3)$$

Where Z_ie is the charge of species i, e denotes the positive elementary charge and $\varepsilon_0\varepsilon_r$ is the dielectric permittivity of the medium (water at 293 K in this case).

The topology of the nanogel is the same as we employed in previous works:[48] 100 polyelectrolyte chains connect through 66 crosslinkers. Inner crosslinkers (40%) were connected to the ends of four polyelectrolyte chains. However, the most external crosslinkers were connected only to three or even two chains. The nanogel lacks chains with a free end. Each chain of the nanogel is formed by 15 monomers whereas the free polyelectrolyte chains are made of 12 or 24 monomers. The bare charge of the nanogel is +100e (one charged group per chain). This is representative sample of a slightly charged

nanogel). As we are interested in charge effects, four families of free chains with different bare charges were employed in our simulations. Linear and ring polyelectrolyte chains with 12 monomers carry bare charges of $-3e$, $-6e$, $-12e$ and $-24e$, whereas the bare charge of linear and ring polyelectrolytes with 24 monomers can be $-4e$, $-8e$, $-16e$, $-24e$ or $-48e$. Figure 1 shows the nanogel and some 24-monomer linear polyelectrolyte chains whose charge is $-8e$.

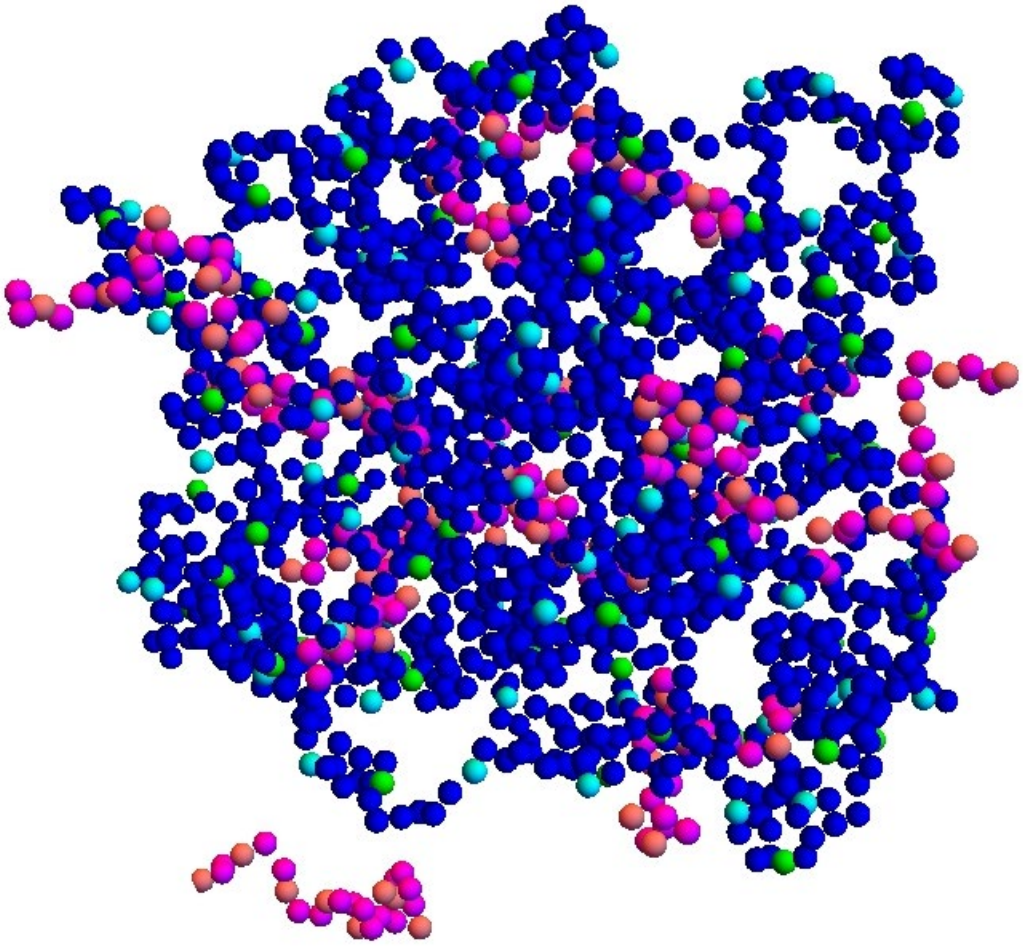

Figure 1. Nanogel and some 24-monomer linear polyelectrolyte chains whose charge is $-8e$. Blue, light blue and green beads represent neutral monomers, charged monomers and crosslinkers of the nanogel. Magenta and pink beads stand for neutral and charged monomers of the polyelectrolyte chains.

The simulation cell contains the cationic nanogel in the middle, a given number of free anionic polyelectrolyte chains and the monovalent anions and cations required to

neutralize the charge of the nanogel and the polyelectrolyte chains, respectively. The simulation box also contains additional cations and anions corresponding to a fixed concentration of monovalent electrolyte (0.1 mM). The length of the cell (L_c) was initially estimated as $L_c \approx 2(R_{NG0} + 3l_D)$, where R_{NG0} is an estimate of the radius of the nanogel in the absence of free polyelectrolyte chains and l_D is the Debye screening length. The definition of l_D is not a trivial issue. In fact, Claudio *et al.* admitted in their pioneering work on coarse-grained simulations of nanogel that different criteria might be employed to define the Debye length.[30] Here we have adopted the simplest criterion: to consider the total number of ionic species in the simulation box (including free polyelectrolyte chains), which gives us a lower bound for the Debye length. After simulation, we confirmed that the cell contained a significant portion of electric double layer around the nanogel. In any case, the cell lengths employed in our simulations were greater than 100 nm.

Monte Carlo (MC) simulations were performed using the canonical ensemble, in which volume, temperature and number of particles are kept constant. Different kinds of MC moves were executed in our simulations according to the conventional Metropolis algorithm: i) 88% of the total number of trial moves are single-particle moves of the beads forming the nanogel and the free polyelectrolyte chains; 10% are translations of the free chains as a whole; iii) 2% are rotations of these free chains. Polyelectrolyte chains were translated and rotated together with their nearest counterions (as if they formed a cluster). Simulations with higher percentages for translations and rotation of free chains were also performed in a preliminary study obtaining almost identical results (within the statistical uncertainty). It should be mentioned, however, that the simulation time considerably increases with these percentages. For that reason, low percentages are preferred. The maximum displacement corresponding to each bead and cluster was individually adjusted so that its respective acceptance ratio was close to 50%. But in the case of clusters, this

maximum displacement could not be larger than the diameter of monomers. Periodic boundary conditions were employed. Long-range Coulomb forces were handled through Ewald sums, which were implemented with the recommendations reported in previous works.[56]

Simulations can be split into three stages. First, the nanogel is equilibrated in the absence of free polyelectrolytes. This stage takes $3 \cdot 10^8$ moves. Then, the polyelectrolyte chains are added to the simulation box and equilibrated ($1 \cdot 10^8$ moves). Finally, a set of statically independent configuration for averaging was extracted from $3 \cdot 10^8$ MC moves. Correlation functions of different properties revealed such configurations should be sampled at least every 10^5 moves (in round numbers). According to this, 3000 statistically independent configurations were obtained. There are efficient simulation packages for coarse-grained models of soft matter, but these simulations were performed using a home-made computer code (in C).

RESULTS AND DISCUSSION

As mentioned previously, four families of free polyelectrolyte chains were employed in our simulations. Figure 2 shows the radius of gyration of all these chains as a function of the magnitude of their bare charge. As can be seen the radius of gyration grows with the bare charge and the number of monomers of the chain. In addition, the two families of linear chains exhibit radii of gyration greater than the families of ring polyelectrolytes with the same number of monomers. This figure also shows that the families of ring chains with 24 monomers and linear chains with 12 monomers exhibit very similar sizes.

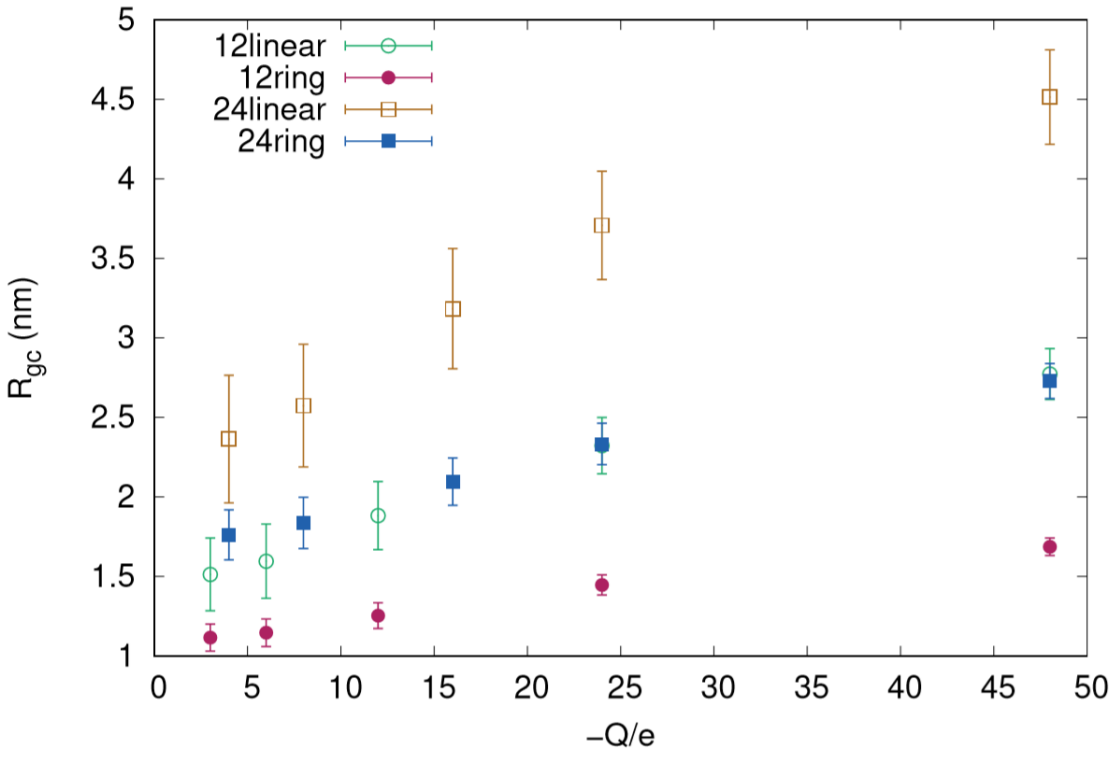

Figure 2. Radius of gyration of the polyelectrolyte chains (R_{gc}) as a function of the magnitude of their charge (in elementary units, $-Q/e$) for: 12-monomer linear chain (open circle), 12-monomer ring chain (closed circle), 24-monomer linear chain (open square), 24-monomer ring chain (closed square).

In a first set of simulations, we employed four polyelectrolyte chains with the same bare charge ($-24e$) but different numbers of monomers (12 or 24) and topology (linear or ring). Figure 3 displays the number of free chains absorbed by the nanogel as a function of the number of chains in the simulation cell, which can also be thought of as the number of chains per nanogel particle in the reservoir. A chain is considered to be absorbed if the distance between its center of mass (CM) and the CM of the nanogel is smaller than its effective radius. Here, the effective radius of the polymer network that constitutes a nanogel (or a complex) is $R_{eff} = \sqrt{5/3}R_g$, where R_g is its radius of gyration.[30,57] It can be shown that the radius of gyration of a solid sphere of radius R is $R_g = \sqrt{3/5}R$. Consequently, R_{eff} provides us an idea of the geometrical radius of the polymer network

considered as a sphere in a first approximation. In fact, an imaginary sphere of radius R_{eff} centered at the CM of the polymer network contains 90% of its monomers.[57] Such an imaginary sphere is also considered the border between the interior and the exterior of the nanogel. As can be inferred from Figure 3, if the number of chains in the simulation cell is small enough (two or four chains in our case), all the chains are absorbed. But if the number of chains in the simulation cell goes on increasing, the number of them absorbed seems to reach a plateau (saturated complexes). This behavior has been experimentally found for complexes formed by poly(*N*-isopropylacrylamide) (PNIPAm) microgels and PDADMAC.[20] It is worth stressing that the maximum number of chains absorbed characterizing the saturated complexes slightly decreases when the radius of gyration increases, as can be concluded comparing Figures 2 and 3.

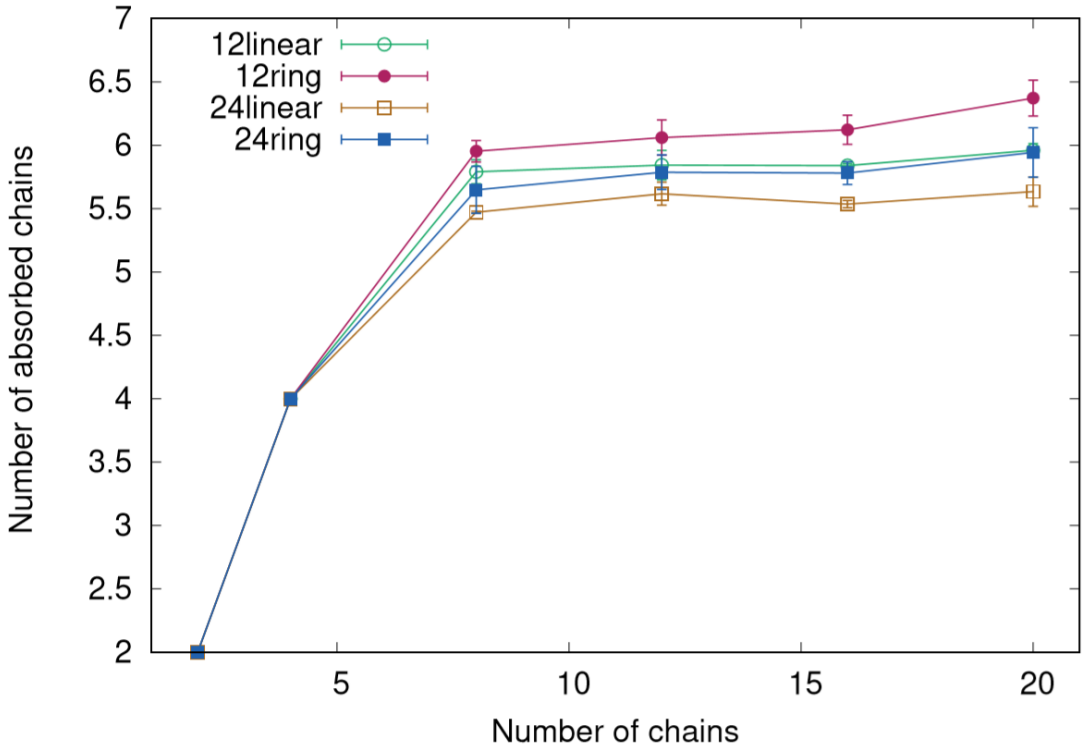

Figure 3. Number of chains absorbed as a function of the number of chains per nanogel for the four chains whose charge is –24*e*: 12-monomer linear chain (open circle), 12-monomer ring chain (closed circle), 24-monomer linear chain (open square), 24-monomer ring chain (closed square).

At this point, it is interesting to find out if the nanogel-polyelectrolyte complexes differ in size from the nanogel. The answer to this question can be found in Figure 4, which shows the effective radius of the complexes as a function of the number of chains absorbed. The error bars were estimated as the standard deviation of the effective diameters obtained in three simulations. A similar criterion was employed for other properties (number of chain absorbed, net charge and electrostatic potential).

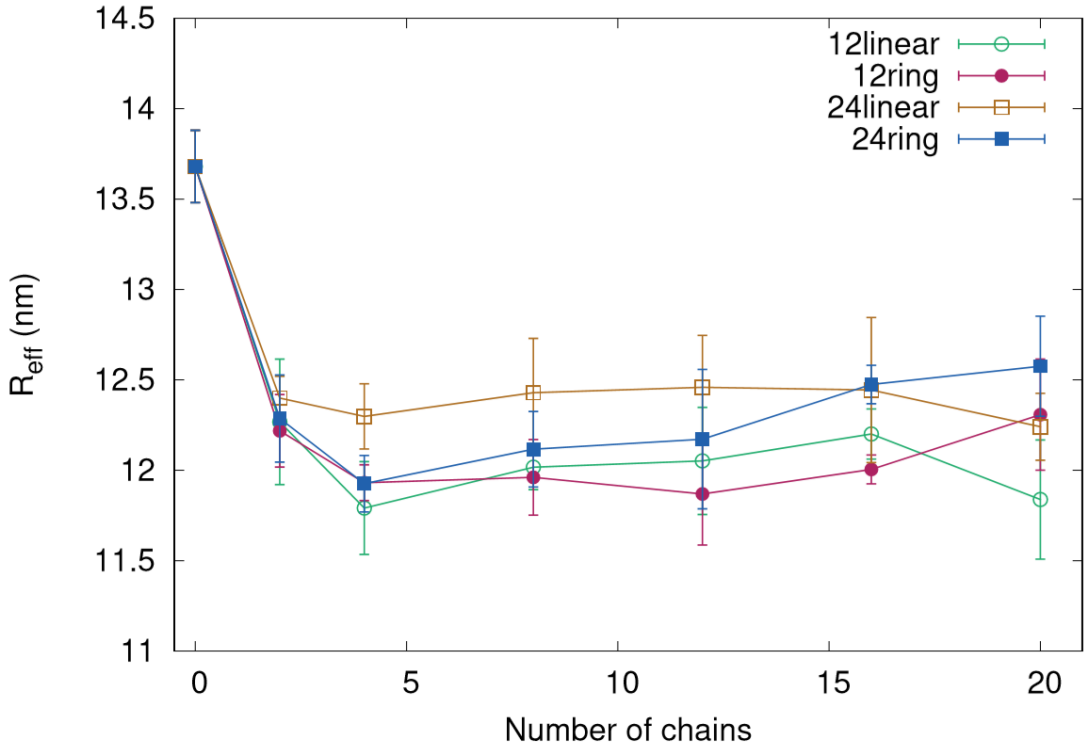

Figure 4. Effective radius of the nanogel-polyelectrolyte complexes as a function of the number of chains in the simulation cell for the four chains whose charge is –24*e*: 12-monomer linear chain (open circle), 12-monomer ring chain (closed circle), 24-monomer linear chain (open square), 24-monomer ring chain (closed square). The radius at 0 is the effective radius of the nanogel in the absence of chains.

As can be seen in Figure 4, first the size of the complexes decreases markedly, then it goes through a minimum and finally it seems to increase slightly. A similar behavior has been reported by Kleinen *et al.*[18] from experiments with microgel-PDADMAC complexes.

The reduction in the size of the polyelectrolyte network observed when the nanogel absorbs just a few chains can be explained as follows. In the absence of chains, the nanogel contains some monovalent counterions that partly neutralize its bare charge. For instance, the bare charge of the nanogel employed in this work is +100*e*, which means that its polymer backbone carries 100 ionized monovalent groups. In addition, the nanogel contains around 22 monovalent counterions. Thus its net charge is +78*e*. When the nanogel absorbs a few highly charged polyelectrolytes, a considerable fraction of these monovalent counterions are expelled, which brings about a fall in the osmotic pressure that swells the polyelectrolyte network, which in turn causes the reduction in size.

Now let us turn our attention to electric properties of these complexes. Figure 5 displays their net charge as a function of the number of chains in the simulation cell for the four polyelectrolytes studied previously. The net charge of the complexes includes the bare charge of the nanogel as well as the charge of the polyelectrolyte chains and small ions inside. As can be seen, the net charge varies from a positive value for the nanogel without chains (+78*e*) to a negative value of the order of −30*e* for saturated complexes. Indeed, the most outstanding feature of this figure is the change of sign in the electric charge. This phenomenon, which has been reported for a wide variety of complex fluids, is known as charge inversion or overcharging.

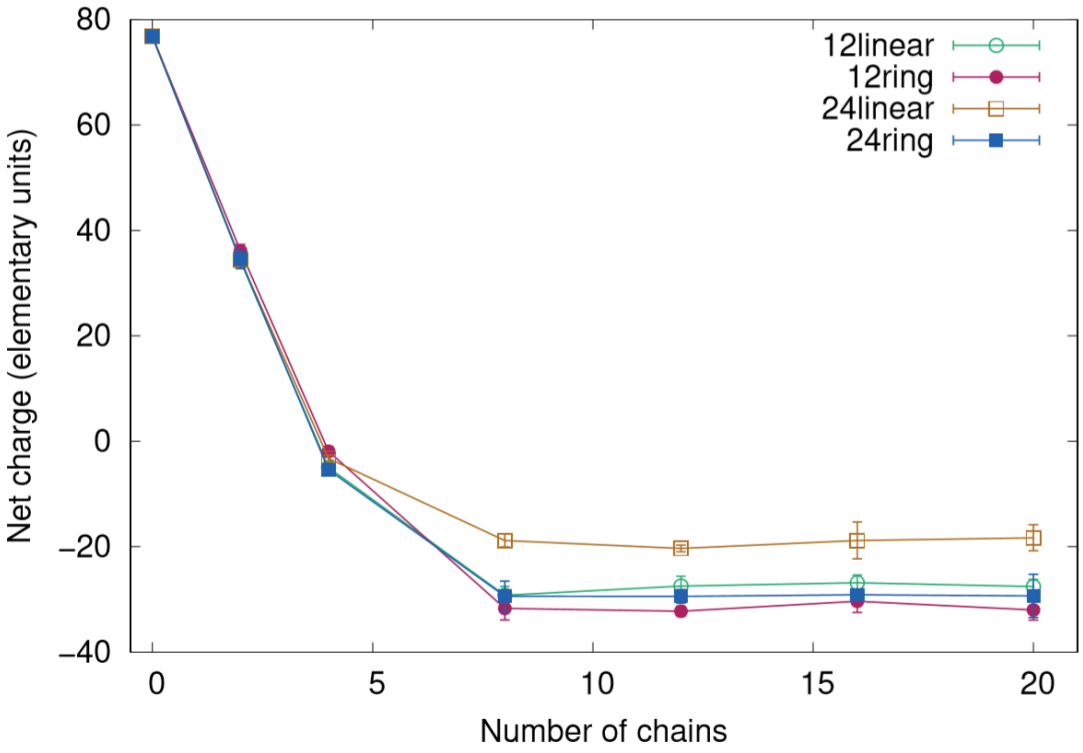

Figure 5. Net charge of the nanogel-polyelectrolyte complexes as a function of the number of chains in the simulation cell for the four chains whose charge is –24*e*: 12-monomer linear chain (open circle), 12-monomer ring chain (closed circle), 24-monomer linear chain (open square), 24-monomer ring chain (closed square). The net charge at 0 is the net charge in the absence of chains.

Figure 5 also shows that the neutralization point is reached when the nanogel absorbs about four polyelectrolyte chains. As each of them carries an electric charge of –24*e*, we can conclude that the charge neutralization can be attributed to these four chains to a great extent. We should also keep in mind that. This can also be mathematically expressed by means of the quotient between the magnitude of the bare charge of the nanogel and the magnitude of the total charge of the absorbed polyelectrolyte. Such a quotient is called nominal charge ratio by some authors.[18,20] In our case, this ratio is around one.

Regarding charge inversion, the question is: why does the nanogel continue to absorb chains beyond the neutralization point? In the last two decades, several mechanisms have been put forward to justify the existence of charge inversion. Previous simulations of

complexes formed by nanogels and hard spherical nanoparticles suggest that strong electrostatic correlations between such nanoparticles can induce charge inversion.[48] Certainly, this idea can also be applied when these nanoparticles are replaced by highly charged polyelectrolyte chains.

Some experiments performed with PDADMAC,[18,20] miktoarm star polymers,[21] polystyrene sulphonate[23] and siRNA[9] have clearly suggested that polyelectrolyte-microgel complexes undergo charge inversion. Nominal charge ratios close to one were also reported. However, it should be stressed that such experiments are based on electrophoretic mobility measurements. In the case of hard colloids, it is well established that electrokinetic properties are directly related to the zeta-potential, the electrostatic potential at the slipping surface, very close to the particle surface. For that reason, we have also computed the dimensionless electrostatic potential at the imaginary border of the nanogel, $e\psi(R_{eff})/k_BT$, where ψ is the electrostatic potential, k_B is Boltzmann's constant and T the absolute temperature. The electrostatic potential at a distance R_{eff} from the CM, $\psi(R_{eff})$, was computed integrating from the border of the simulation cell to R_{eff}:

$$\psi(R_{eff}) = -\int_{L_c/2}^{R_{eff}} E(r)dr \qquad (4)$$

Here $E(r)$ is the spherically averaged electric field at a distance r from the CM, which in turn can be obtained from the net charge enclosed by a sphere of radius r by applying Gauss' law.

Figure 6 shows the dimensionless electrostatic potential as a function of the number of chains. The error bars were computed as the standard deviation of the ψ-values obtained in three simulations. As expected, the electrostatic potential also exhibits a change of sign for saturated complexes, which would be straightforwardly related to an inversion in the electrophoretic mobility detected in experiments. It should also be mentioned that the

electrostatic potential does not depend on the topology of the complexes. This behavior contrasts with that found for lipoplexes (complexes formed by liposomes and DNA). The charge of ionic liposomes is mainly placed on their surface and the complexation of DNA by liposomes results in complexes in which the topology of nucleic acid molecules plays an important role.[49,50]

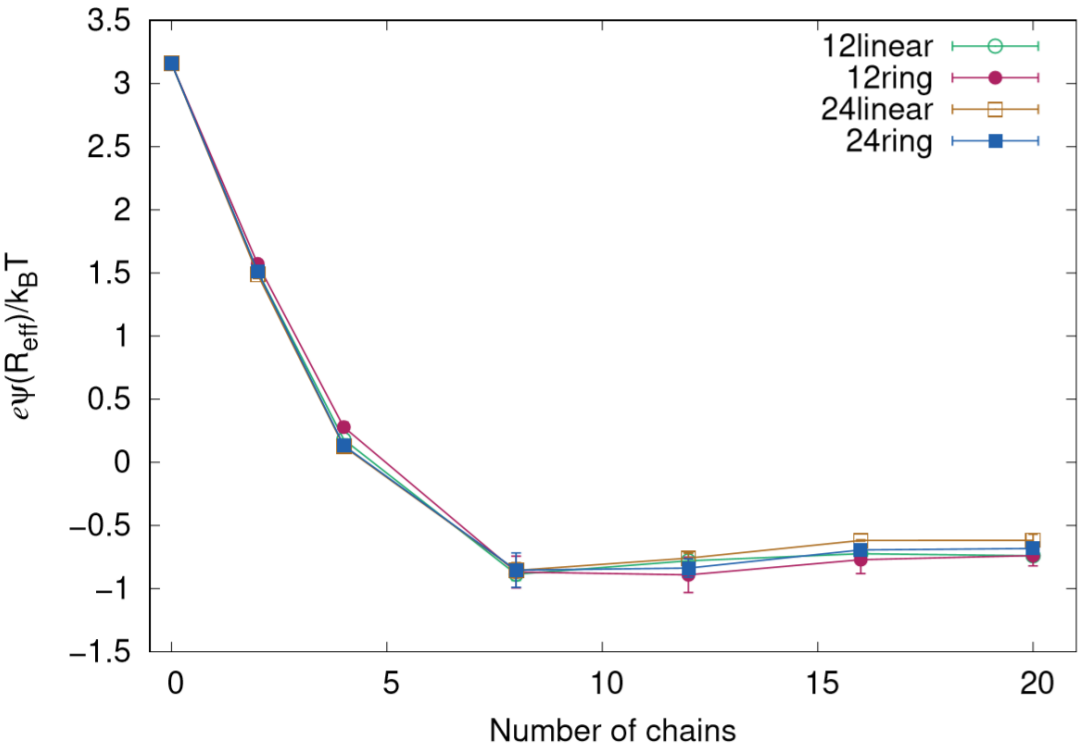

Figure 6. Dimensionless electrostatic potential at the imaginary surface of the nanogel-polyelectrolyte complexes as a function of the number of chains per nanogel in the reservoir for the four chains whose charge is –24*e*: 12-monomer linear chain (open circle), 12-monomer ring chain (closed circle), 24-monomer linear chain (open square), 24-monomer ring chain (closed square). The dimensionless electrostatic potential at 0 is the net charge in the absence of chains.

So far, we have commented results of simulations in which the polyelectrolyte chains had the same charge (–24*e*). It would be interesting to analyze how the electrostatic potential depends on the charge of the chains. In practice, this could be the case of polyelectrolytes with weak acid/basic groups, whose charge varies with pH. Consequently, simulations were performed with the four families of polyelectrolytes but setting the number of chains

in the simulation cell to 20. Figure 7 displays the normalized electrostatic potential obtained for the four families of chains as a function of their electric charge.

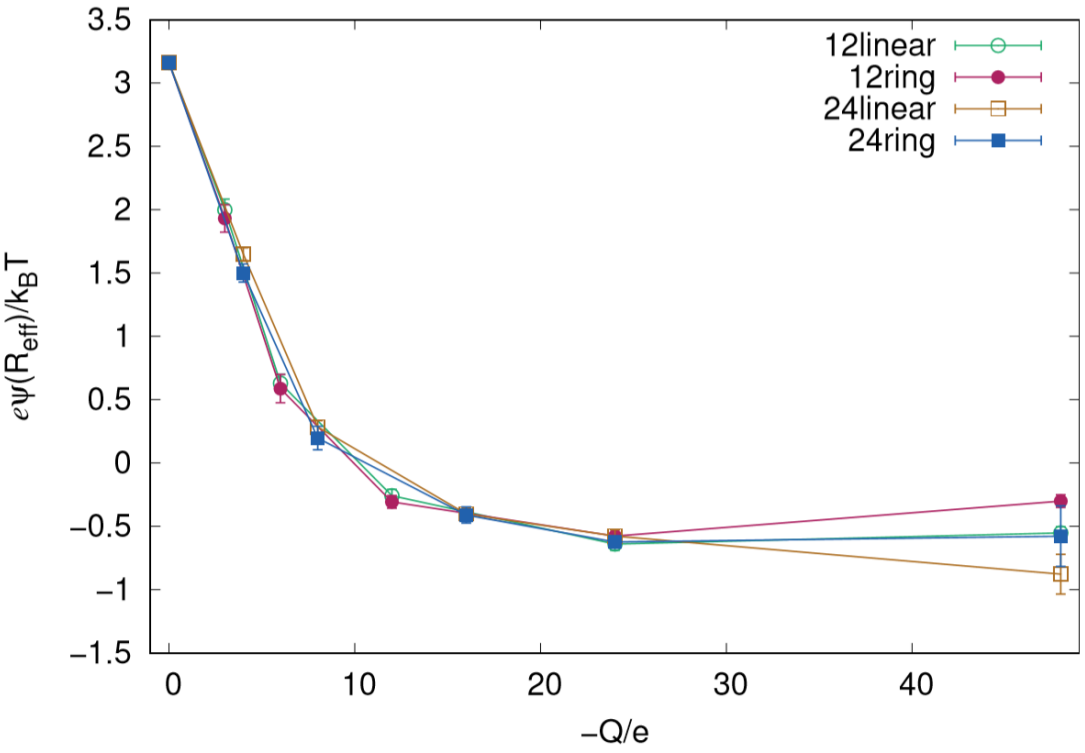

Figure 7. Dimensionless electrostatic potential at the imaginary surface of the nanogel-polyelectrolyte complexes as a function of the chain charge for: 12-monomer linear chains (open circle), 12-monomer ring chains (closed circle), 24-monomer linear chains (open square), 24-monomer ring chains (closed square). The value at 0 stands for the normalized electrostatic potential in the absence of chains.

This figure clearly shows that the electrostatic potential of the complexes exhibits inversion only if the magnitude of the charge of chains is greater than 10*e*. This threshold seems to be similar for the four families of polyelectrolytes simulated here and it is also very close to the charge required for inversion in nanogel-nanoparticles composites with sizes ranging from 2 to 6 nm previously simulated.[48] This suggests that the charge required for inversion of several species encapsulated by a nanogel is not very sensitive to the charge distribution since polyelectrolytes chains with different lengths and topology and spherical nanoparticles exhibit similar values. The net charge also displays a threshold of about 10*e* for charge inversion (figure not shown).

Finally, it is quite instructive to analyze where the polyelectrolyte chains encapsulated by the nanogel are located (depending on their charge). In fact, Gelissen *et al.* has recently employed simulations to compute the distribution of polystyrene sulphonate chains inside polyampholyte core-shell microgels.[23] In our case, Figure 8 and 9 show the spherically averaged local chain number density, $\rho_{ch}(r)$, as a function of chain-nanogel center-to-center distance r for different polyelectrolyte chains of 12 (Figure 8) and 24 (Figure 9) monomers per chain. The most remarkable feature of both figures is that the preferential location of the chains inside the nanogel strongly depends on their electric charge. Chains with charges (in magnitude) smaller than $10e$ are preferentially located at the center of the nanogel. Chains with $-3e$, $-4e$, $-6e$ or $-8e$ are illustrative examples of this behavior. In contrast, chains with greater charges leave empty the center of the nanogel and are structured in shells at different distances from it. Given that the threshold charge for inversion in the electrostatic potential is $-10e$ we can also state that the distribution of chains inside the nanogel strongly depends on the existence of charge inversion in the complex.

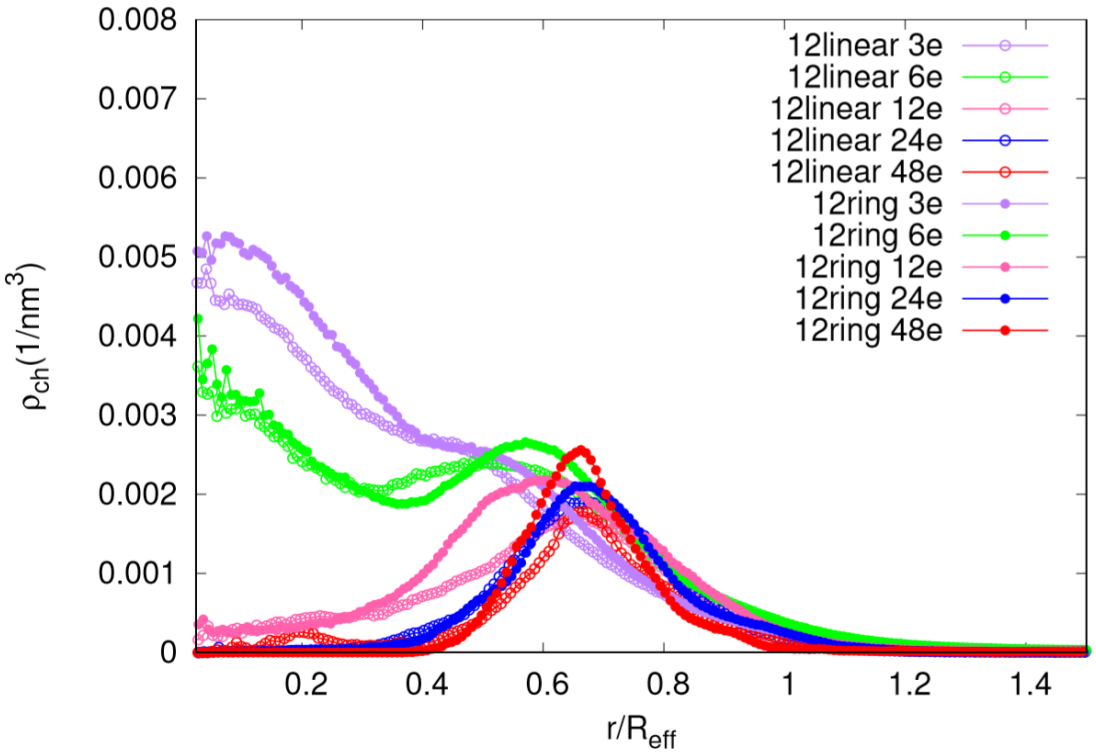

Figure 8. Spherically averaged local chain number density, $\rho_{ch}(r)$, as a function of the chain-nanogel center-to-center distance r for linear and ring polyelectrolytes of 12 monomers per chain.

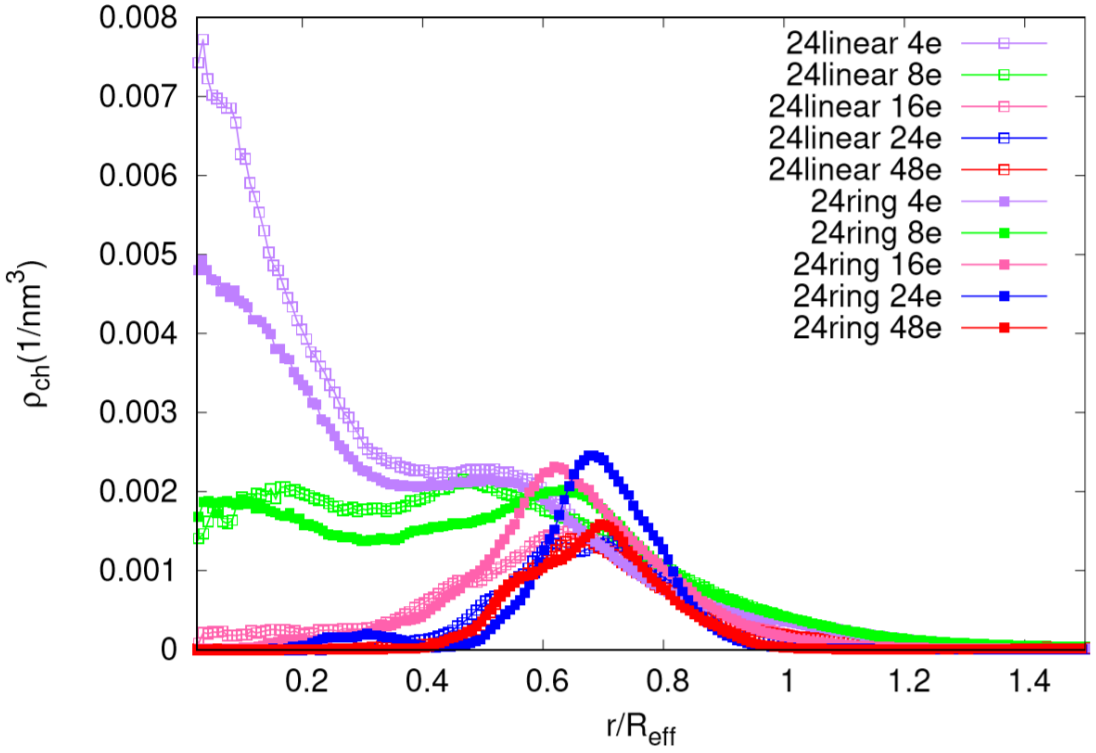

Figure 9. Spherically averaged local chain number density, $\rho_{ch}(r)$, as a function of the chain-nanogel center-to-center distance r for linear and ring polyelectrolytes of 24 monomers per chain.

CONCLUSIONS

In this work, we have performed coarse-grained Monte Carlo simulations of complexes formed by a nanogel and oppositely charged polyelectrolyte chains with different charge, number of monomers per chain and topology. Given that the model employed only involves nonspecific forces (electrostatic and excluded volume forces), the results can be extrapolated to a wide variety of nanogel-polyelectrolyte complexes to a great extent. Special attention has been paid to two phenomena observed in experiments with microgel-polyelectrolyte complexes: the deswelling and charge inversion undergone after absorption.

Our results reveal that the net charge of the complexes and their surface electrostatic potential are almost identical for linear and ring chains. In other words, the topology of the polyelectrolytes has little or no influence on many of these properties. This also implies that distribution of charge in polyelectrolyte chains is not a determining feature in phenomena such as charge inversion or the reduction of the complex size after absorbing some chains.

According to our results, charge inversion only takes place if the charge of the polyelectrolytes exceeds a threshold value, which suggests that strong electrostatic correlations between highly charged polyelectrolyte chains are responsible for such a phenomenon. It should be also stressed that the existence of charge inversion has a profound influence on the distribution of chains inside the nanogel. Slightly charged polyelectrolytes are preferentially located in the center of the nanogel. However, highly charged chains (which give rise to charge inversion) leave empty the center of the nanogel and form shells at different distances from it.

CONFLICTS OF INTEREST.

There are no conflicts of interest to declare.

ACKNOWLEDGEMENTS.

The authors thank the financial support from the following institutions: i) ‘Ministerio de Economía y Competitividad, Plan Estatal de InvestigaciónCientífica y Técnica y de Innovación 2013-2016’, Project FIS2016-80087-C2-2-P; ii) European Regional Development Fund (ERDF).

REFERENCES

1 R. Pelton, *Adv. Colloid Interface Sci.*, 2000, **85**, 1–33.

2 S. Seiffert, *J. Polym. Sci. Part A Polym. Chem.*, 2014, **52**, 435–449.

3 M. D. Blanco, S. Guerrero, C. Teijón, R. Olmo, L. Pastrana, I. Katime and J. M. Teijón, *Polym. Int.*, 2008, **57**, 1215–1225.

4 A. V Kabanov and S. V Vinogradov, *Angew. CHEMIE-INTERNATIONAL Ed.*, 2009, **48**, 5418–5429.

5 J. K. Oh, R. Drumright, D. J. Siegwart and K. Matyjaszewski, *Prog. Polym. Sci.*, 2008, **33**, 448–477.

6 K. Raemdonck, J. Demeester and S. De Smedt, *Soft Matter*, 2009, **5**, 707–715.

7 M. Karg, A. Pich, T. Hellweg, T. Hoare, L. A. Lyon, J. J. Crassous, D. Suzuki, R. A. Gumerov, S. Schneider, I. I. Potemkin and W. Richtering, *Langmuir*, 2019, **35**, 6231–6255.

8 T. Casalini and G. Perale, *Gels*, 2019, 5, 28.

9 A. Tamura, M. Oishi and Y. Nagasaki, *Biomacromolecules*, 2009, **10**, 1818–1827.

10 W. H. Blackburn, E. B. Dickerson, M. H. Smith, J. F. McDonald and L. A. Lyon, *Bioconjug. Chem.*, 2009, **20**, 960–968.

11 R. Sunasee, P. Wattanaarsakit, M. Ahmed, F. B. Lollmahomed and R. Narain, *Bioconjug. Chem.*, 2012, **23**, 1925–1933.

12 M. Ahmed, P. Wattanaarsakit and R. Narain, *Polym. Chem.*, 2013, **4**, 3829–3836.

13 C. Vauthier, C. Zandanel and A. L. Ramon, *Curr. Opin. Colloid Interface Sci.*, 2013, **18**, 406–418.

14 S. L. Goh, N. Murthy, M. Xu and J. M. J. Fréchet, *Bioconjug. Chem.*, 2004, **15**, 467–474.

15 E. Mauri, G. Perale and F. Rossi, *ACS Appl. Nano Mater.*, 2018, **1**, 6525–6541.

16 D. Huang, H. Qian, H. Qiao, W. Chen, J. Feijen and Z. Zhong, *Expert Opin. Drug Deliv.*, 2018, **15**, 703–716.

17 R. Kandil and O. M. Merkel, *Curr. Opin. Colloid Interface Sci.*, 2019, **39**, 11–23.

18 J. Kleinen and W. Richtering, *Macromolecules*, 2008, **41**, 1785–1790.

19 J. Kleinen and W. Richtering, *J. Phys. Chem. B*, 2011, **115**, 3804–3810.

20 J. Kleinen and W. Richtering, *Colloid Polym. Sci.*, 2011, **289**, 739–749.

21 S. Walta, D. V. Pergushov, A. Oppermann, A. A. Steinschulte, K. Geisel, L. V. Sigolaeva, F. A. Plamper, D. Wöll and W. Richtering, *Polymer (Guildf).*, 2017, **119**, 50–58.

22 H. Bysell, P. Hansson and M. Malmsten, *J. Phys. Chem. B*, 2010, **114**, 7207–7215.

23 A. P. H. Gelissen, A. Scotti, S. K. Turnhoff, C. Janssen, A. Radulescu, A. Pich, A. A. Rudov, I. I. Potemkin and W. Richtering, *Soft Matter*, 2018, **14**, 4287–4299.

24 W. M. Gelbart, R. F. Bruinsma, P. A. Pincus and V. A. Parsegian, *Phys. Today*, 2000, **53**, 38–44.

25 Y. Levin, *Reports Prog. Phys.*, 2002, **65**, 1577–1632.

26 A. Y. Grosberg, T. T. Nguyen and B. I. Shklovskii, *Rev. Mod. Phys.*, 2002, **74**, 329–345.

27 M. Quesada-Perez, E. Gonzalez-Tovar, A. Martin-Molina, M. Lozada-Cassou and R. Hidalgo-Alvarez, *CHEMPHYSCHEM*, 2003, **4**, 234–248.

28 Y. Levin, *BRAZILIAN J. Phys.*, 2004, **34**, 1158–1176.

29 J. Faraudo and A. Martin-Molina, *Curr. Opin. Colloid Interface Sci.*, 2013, **18**, 517–523.

30 G. C. Claudio, K. Kremer and C. Holm, *J. Chem. Phys.*, 2009, **131**, 094903.

31 P. K. Jha, J. W. Zwanikken, F. A. Detcheverry, J. J. de Pablo and M. O. de la Cruz, *Soft Matter*, 2011, **7**, 5965–5975.

32 L. Rovigatti, N. Gnan and E. Zaccarelli, *J. PHYSICS-CONDENSED MATTER*, , DOI:10.1088/1361-648X/aaa0f4.

33 L. Rovigatti, N. Gnan, L. Tavagnacco, A. J. Moreno and E. Zaccarelli, *Soft Matter*, 2019, **15**, 1108–1119.

34 A. Martín-Molina and M. Quesada-Pérez, *J. Mol. Liq.*, 2019, **280**, 374–381.

35 E. S. Minina, P. A. Sánchez, C. N. Likos and S. S. Kantorovich, *J. Mol. Liq.*, 2019, **289**, 111066.

36 T. Colla, R. Blaak and C. N. Likos, *Soft Matter*, 2018, **14**, 5106–5120.

37 T. Colla, P. S. Mohanty, S. Nojd, E. Bialik, A. Riede, P. Schurtenberger and C. N. Likos, *ACS Nano*, 2018, **12**, 4321–4337.

38 J. Riest, L. Athanasopoulou, S. A. Egorov, C. N. Likos and P. Ziherl, *Sci. Rep.*, , DOI:10.1038/srep15854.

39 H. Lowen, A. Esztermann, A. Wysocki, E. Allahyarov, R. Messina, A. Jusufi, N. Hoffmann, D. Gottwald, G. Kahl, M. Konieczny and C. N. Likos, in *Kinetic Theory of Nonideal Plasmas*, ed. Bonitz, M and Kraeft, WD, IOP PUBLISHING LTD, DIRAC HOUSE, TEMPLE BACK, BRISTOL BS1 6BE, ENGLAND, 2005, vol. 11, pp. 207–222.

40 M. Quesada-Perez and A. Martin-Molina, *Soft Matter*, 2013, **9**, 7086–7094.

41 M. Quesada-Pérez, S. Ahualli and A. Martín-Molina, *J. Chem. Phys.*, 2014, **141**, 124903.

42 R. Schroeder, A. A. Rudov, L. A. Lyon, W. Richtering, A. Pich and I. I. Potemkin, *Macromolecules*, 2015, **48**, 5914–5927.

43 H. Kobayashi and R. Winkler, *Polymers (Basel).*, 2014, **6**, 1602–1617.

44 A. Moncho-Jorda and I. Adroher-Benitez, *Soft Matter*, 2014, **10**, 5810–5823.

45 H. Kobayashi and R. G. Winkler, *Sci. Rep.*, , DOI:10.1038/srep19836.

46 H. Kobayashi, R. Halver, G. Sutmann and R. G. Winkler, *Polymers (Basel).*

47 N. Gnan, L. Rovigatti, M. Bergman and E. Zaccarelli, *Macromolecules*, 2017, **50**, 8777–8786.

48 M. D. M. Ramos-Tejada and M. Quesada-Pérez, *Macromolecules*, 2019, **52**, 2223–2230.

49 M. Muñoz-Úbeda, S. K. Misra, A. L. Barrán-Berdón, C. Aicart-Ramos, M. B. Sierra, J. Biswas, P. Kondaiah, E. Junquera, S. Bhattacharya and E. Aicart, *J. Am. Chem. Soc.*, 2011, **133**, 18014–18017.

50 M. Muñoz-Úbeda, A. Rodríguez-Pulido, A. Nogales, O. Llorca, M. Quesada-Pérez, A. Martín-Molina, E. Aicart and E. Junquera, *Soft Matter*, 2011, **7**, 5991.

51 M. Quesada-Pérez, I. Adroher-Benítez and J. A. Maroto-Centeno, *J. Chem. Phys.*, 2014, **140**, 204910.

52 S. Schneider and P. Linse, *J. Phys. Chem. B*, 2003, **107**, 8030–8040.

53 S. Schneider and P. Linse, *Macromolecules*, 2004, **37**, 3850–3856.

54 S. Edgecombe, S. Schneider and P. Linse, *Macromolecules*, 2004, **37**, 10089–10100.

55 B. A. Mann, C. Holm and K. Kremer, *J. Chem. Phys.*, , DOI:15490310.1063/1.1882275.

56 M. Quesada-Perez and A. Martin-Molina, *Soft Matter*, 2013, **9**, 7086–7094.

57 S. Ahualli, A. Martin-Molina, J. Alberto Maroto-Centeno and M. Quesada-Perez, *Macromolecules*, 2017, **50**, 2229–2238.